

EXPERIMENTAL INVESTIGATION OF HEAT TRANSFER ENHANCEMENT IN A MICROTUBE USING NANOFLUIDS

B.H. Salman^{a*}, H. A. Mohammed^b, A. Sh. Kherbeet^c, R. Saidur^d

^{*}Author for correspondence

^a *FABE, Limkokwing University of Creative Technology, Cyberjaya, 63000, Malaysia*

^b *Department of Thermofluids, Faculty of Mechanical Engineering, Universiti Teknologi Malaysia, 81310 UTM Skudai, Johor Bahru, Malaysia*

^c *Mechanical Engineering Department, College of Engineering, Universiti Tenaga Nasional, Jalan IKRAM-UNITEN, 43000 Kajang, Selangor, Malaysia*

^d *Department of Mechanical Engineering, University of Malaya, 50603 Kuala Lumpur, Malaysia*

E-mail: Bh.salman@limkokwing.edu.my

ABSTRACT

Forced convective laminar flow of different types of nanofluids such as Al₂O₃ and SiO₂, with nanoparticle size 30 nm, and different volume fractions ranged from 0.5% to 1% using water as base fluids was investigated experimentally. The Microtube (MT) with 0.01 cm diameter and 20 cm length is used in this investigation. This investigation covers Reynolds number in the range of 90 to 800. The results have shown that SiO₂-water nanofluid has the highest Nusselt number, followed by Al₂O₃-water, and lastly pure water. The maximum heat transfer enhancement was about 22% when using the nanofluids and the experimental results agree well with the conventional theory.

1 INTRODUCTION

In the last few years, the fast growth of research in the heat transfer area was improved by using new kind of heat transfer fluids called nanofluids which have nanosized particles. These particles can be metallic or nonmetallic such as Al₂O₃, CuO, SiO₂, TiO₂, Cu, Ni, Al and ZnO. Most of the recent studies showed that solid nanoparticles with high thermal conductivity when suspended in the base fluid would enhance the convective heat transfer coefficient and the effective thermal conductivity of the base fluid [1-8] and [26].

Large number of experimental and numerical studies focused on the flow and heat transfer behavior in a microtube has been reported by many researchers, Liu et al.

[9] investigated experimentally the forced convective heat transfer characteristics in quartz microtubes with inner diameters of 242, 315 and 520 μm. The deionized water was used as the working fluid. The Reynolds number was ranged from 100 to 7000. The results indicate that the experimental Nusselt number tends to be in agreement with that of the laminar correlations when the flow state was laminar.

Zhou et al. [10] investigated experimentally and numerically the flow and heat transfer characteristics of liquid laminar flow in MT. They used smooth fused silica and rough stainless steel microtubes with the hydraulic diameters of 50–100 μm and 373–1570 μm, respectively. Deionized water was used as the working fluid. The Reynolds numbers were ranged from 20 to 2400. The results show that the Nusselt number along the axial direction do not accord with the conventional results especially when the Reynolds number is low and the relative tube wall thickness is high.

Lelea [11] investigated numerically the conjugate heat transfer and laminar fluid flow in a stainless steel microtube. Three different fluids with temperature dependent fluid properties, water and two dielectric fluids, HFE-7600 and FC-70 were used. The diameter ratio of the MT was Di/Do=0.1/0.3 mm with a tube length L=70 mm. The Reynolds number range was less than 400. The results indicate that thermal conductivity has a significant influence on the local Nu number behavior as long as the Re number was low.

Celata et al. [12] investigated experimentally the influence of channel wall roughness and the channel wall hydrophobicity on adiabatic flow in circular microchannels. Different diameters of MT range from 70 μm to 326 μm were used with Reynolds number less than 300 for all diameters. The results indicate that, with degassed water, there was no

effect of slip flow noted due to hydrophobic channel walls even at 70 μm inner diameter. For roughened glass channels, an increased in friction factor above $64/Re$ was observed only at the smallest diameter of 126 μm .

Peng et al. [13] investigated water flow in a fused glass microtube with an inner diameter of 230 μm and an outer diameter of 500 μm . The Reynolds number was ranged from 1540 to 2960. The results indicate that the flow transition from laminar to turbulent occurs at Reynolds number 1700 to 1900, and the turbulence becomes fully developed at $Re > 2500$.

NOMENCLATURE

| | | |
|-------------------------|--|---|
| Al_2O_3 | | Aluminium oxide |
| A | m^2 | Area of the test tube |
| c_p | $(\text{J}/(\text{kg}\cdot\text{K}))$ | Specific heat of water |
| D | μm | Diameter of test tube |
| D_h | μm | Hydraulic diameter of test tube |
| f | | Darcy friction factor |
| h_x | $(\text{W}/(\text{m}^2\cdot\text{K}))$ | Local heat transfer coefficient |
| \dot{m} | kg/s | Mass flow rate |
| Nu_x | | Nusselt number |
| Δp | | Pressure drop |
| q | (W / m^2) | Heat flux |
| Q | (W) | Heat transfer rate |
| Re | | Reynolds number |
| R | | Radius of test tube |
| SiO_2 | | Silicon oxide |
| T | (K) | Temperature |
| T_{w_x} | (K) | Wall temperature along x-direction |
| $T_{b,x,int}$ | | Bulk temperature |
| ΔT_x | (K) | Bulk temperature difference along x-direction |
| U | (V) | Voltage supply |
| U_R | | Uncertainty |
| I | (A) | Electric current |
| τ_w | | Wall shear stress |

Greek symbols

| | | |
|--------|--------------------------|---------------|
| ρ | (kg/m^3) | Fluid density |
| Φ | (W) | Power supply |

Subscripts

| | |
|------------|----------------------|
| <i>ave</i> | Average |
| <i>b</i> | Bulk temperature |
| <i>c</i> | Cross-section |
| <i>i</i> | Inner of test tube |
| <i>in</i> | Inlet |
| <i>int</i> | Linear interpolation |
| <i>l</i> | Liquid |
| <i>o</i> | Outer of test tube |
| <i>w</i> | Wall surface |

Mala and Li [14] investigated experimentally the effects of water flow in microtube. Fused silica (FS) and stainless steel (SS) of MT were used. The diameters used were ranged from 50 to 254 μm with Reynolds number up to 2500. The results revealed that as the Reynolds number increased, a significant deviation from the conventional theory was observed. In addition, the friction factor and the friction constant were higher than that predicted by the conventional theory.

Wen and Ding [15] investigated experimentally the effects of convective heat transfer of nanofluids at the entrance region of the copper tube with 970 mm length. The de-ionized water with Al_2O_3 nanoparticle was used as working fluids. Reynolds number used was ranged from 500 to 2100. The results indicate that the use of Al_2O_3 significantly enhanced the convective heat transfer in the laminar flow regime and this enhancement increased with Reynolds number and the particle concentration.

Koo and Kleinstreuer [16] investigated experimentally the effects of viscous dissipation on the temperature field and the friction factor in a microtube (MT) and microchannel (MC). Three working fluids were used, water, methanol and iso-propanol. The results indicated that the viscous dissipation effect on the friction factor was increased as the system size decreased. For water flow in a tube with diameter 50 μm , viscous dissipation becomes significant. For liquids, the viscous dissipation effects decreased as the fluid temperature increased.

Lelea and Cioabla [17] investigated numerically the effects of viscous dissipation on heat transfer and fluid flow in microtubes. Three different fluids, water and two dielectric fluids, HFE-7600 and FC-70 were used. The diameter ratio of the MT was 0.33 with a tube length $L=100$ mm. Two different heat transfer conditions, cooling and heating and three different Brinkman number 0.01, 0.1 and 0.5 were used. The results revealed that the friction factor and Poiseuille constant Po are affected at $Br=0.5$ for water and start with $Br=0.1$ for highly viscous fluids HFE-7600 and FC-70. The Nusselt number for the cooling case for $Br=0.5$ was about three times higher than for heating case, regardless with the fluid type.

Minea [18] investigated numerically the turbulent convective heat transfer in a two-dimensional microtube with 10 mm diameter and variable length with constant heating temperature. Water- Al_2O_3 nanofluids with different volume fractions ranged from 1% to 4% were used. This investigation covers Reynolds number in the range of 10^4 - 10^5 . The results have shown that the convective heat transfer coefficient for a nanofluid is enhanced than that of the base liquid. Wall heat transfer flux is increased with the particle volume concentration and Reynolds number.

Minea [19] investigated numerically the effect due to the uncertainty in the values of the physical properties of water- Al_2O_3 nanofluid on their thermo hydraulic performance for laminar fully developed forced convection in a two zones tube. The results revealed that the heat transfer coefficient of Al_2O_3 /water nanofluids is increased by 3.4-27.8% under fixed Reynolds number compared with that of pure water.

Kang et al. [20] investigated experimentally the thermal performance using nanofluids and conventional fluids. The

nanofluid used was an aqueous solution of 10 and 35 nm diameter silver nano-particles. The results show that the temperature difference decreased from 0.56 to 0.65 °C when using the nanofluids compared to DI-water.

Moraveji and Esmaeili [21] investigated numerically forced convection heat transfer with laminar and developed flow for water-Al₂O₃ nanofluid inside a circular tube with diameter 10 mm under constant heat flux from the wall. Nanofluids with size particles equal to 100 nm and particle concentrations of 1 and 4 wt% were used. The result shows that the heat transfer was enhanced by increasing the concentration of nanoparticles in nanofluid and Reynolds number.

Akbarinia et al. [22] investigated numerically the laminar mixed convection heat transfer in a circular curved tube with diameter 0.02 m with a nanofluid consisting of water and 1 vol. % Al₂O₃ at different inclination angles. The results reveal that the heat transfer coefficient increased by 15% at 4 Vol. % Al₂O₃. Skin friction coefficient continually increased with the tube inclination, but the heat transfer coefficient reached a maximum at the inclination angle of 45°

Wu et al. [23] investigated experimentally the pressure drop and heat transfer characteristics of alumina/water nanofluids in helical heat exchangers with diameter 13.28 mm at Reynolds number ranged from 1000-15000. The results reveal that the heat transfer enhancement of the nanofluids compared to water is from 0.37% to 3.43%.

To the best of the authors' knowledge, the number of studies reported in the previous literature related to a microtube (MT) using nanofluids are very limited, and that has motivated this investigation. In this paper, laminar forced convective heat transfer in a microtube with different types of nanofluids with different nanoparticle volume fractions was experimentally investigated. This investigation covers Reynolds number in the range of 90 to 800 and particle diameters of 30 nm. Results of interest such as the Nusselt number, friction factor, effects of nanoparticles type and volume fraction are reported.

2 EXPERIMENTAL SETUP AND PROCEDURE

2.1. EXPERIMENTAL SETUP

The nanoparticles used in this work were Al₂O₃ and SiO₂ with size of 30 nm. The base working fluid was pure water. In this work the two step method is used to prepare the nanofluids. The amount of the nanoparticle required for preparation of nanofluids is calculated using the mixture formula. A sensitive balance (HR-250 az) with 0.1 mg resolution is used to weight the nanoparticles very accurately. The weight of the nanoparticles required for preparation of 100 ml of Al₂O₃ and SiO₂ nanofluids of a particular volume concentration, using water as base fluid is calculated by using the following relation [24].

$$\text{volume concentration, } \phi \% = \frac{\left[\frac{w_{\text{particle}}}{\rho_{\text{particle}}} \right]}{\left[\frac{w_{\text{particle}}}{\rho_{\text{particle}}} + \frac{w_{\text{basefluid}}}{\rho_{\text{basefluid}}} \right]} \quad (1)$$

The amount of SiO₂ and Al₂O₃ nanoparticles required to prepare nanofluids of different percentage volume concentration in 100 ml of base fluid is summarized in table 1.

Table 1: volume concentrations of SiO₂ and Al₂O₃ nanoparticles with corresponding weight

| N O. | Volume concentration, ϕ % | Weight of nanoparticles ($W_{Al_2O_3}$), grams | Weight of nanoparticles (W_{SiO_2}), grams |
|------|--------------------------------|--|--|
| 1 | 0.005 | 2 | 1.11 |
| 2 | 0.01 | 4.05 | 2.248 |

In the present investigation, neither surfactants nor acid are added in the nanofluids, because with the addition of surfactants the thermo physical properties of nanofluids are affected. Addition of acid may damage the tube material because corrosion takes place after a few days with the prolonged usage of such nanofluids in practical applications. All the test samples of Al₂O₃ and SiO₂ nanofluids used were subjected to ultrasonic shaker for about 30 minutes for each 100 ml. after using the ultrasonic shaker for nanofluids, the shaker incubator (upright double deck shaking incubator) was used to shaking the nanofluids till the total amount of nanofluids is obtained that is used in this experiment.

The Al₂O₃ and SiO₂ nanofluids samples thus prepared are kept for observation and no particle settlement was observed at the bottom of the flask containing Al₂O₃ and SiO₂ nanofluids even after five hours. In the present experiments with the nanofluids, the time taken to complete the experiment for property estimation is less than the time required for first sedimentation to take place. Hence surfactants are not mixed in the nanofluids. The nanofluids prepared assumed to be an isentropic, Newtonian in behavior and their thermo physical properties was measured for the nanofluids samples. However, the nanofluids experimental properties for the SiO₂ 1% +H₂O, SiO₂ 0.5% +H₂O and Al₂O₃ 1% +H₂O is shown in Table 2.

Table 2: The Experimental Thermophysical Properties

| Properties | SiO ₂ 1%+H ₂ O | Al ₂ O ₃ 1%+H ₂ O | SiO ₂ 0.5%+H ₂ O |
|------------------------------|--------------------------------------|--|--|
| Thermal Conductivity [W/m.K] | 0.629 | 0.664 | 0.6288 |
| Density [Kg/m ³] | 1010 | 1024 | 1003 |
| Viscosity [Pa.s] | 0.001090415 | 0.001112082 | 0.001030322 |
| Specific Heat [J/Kg K] | 4166.188 | 4175.66 | 4170.444 |

The experimental system used was composed of three main systems: the pressurizing system, the heating system, and the data acquisition system. The experimental system is shown in figure 1.

For the pressurizing system, an compressed nitrogen tank and water/ nanofluids holding tank were used to create pressure to drive the flow through the MT. This setup provided a smoother and more stable flow of water/ nanofluids than a pump would have provided. The compressed nitrogen tank (rated for 200 psi) was fitted with a control valve and pressure regulator. This allowed for the pressure of the nitrogen leaving the tank to be monitored and adjusted while also monitoring the pressure of the nitrogen still in the tank. The 5 liters water/ nanofluids holding tank was connected to the compressed nitrogen tank with a plastic tube. The compressed nitrogen entered the water/ nanofluids holding tank from the upper inlet side, and this kept the water holding tank pressurized. With this tank pressurized, the water could be forced through another plastic tube coming out of the bottom of the water holding tank. Two pressure gauges at the inlet and the outlet of the microtube were used to release the pressure of the water/ nanofluids that is coming from the holding tank.

The MT was instrumented with thermocouples and pressure gauge to monitor the fluid flow and heat transfer through the MT. The thermocouples used were placed in 5 different places along the MT wall at a distance of 3mm from the MT. Inlet and outlet temperatures was measured using 2 more thermocouples placed at the inlet and outlet of the MT.

The MT inlet and outlet was fitted with copper sump to allow the plastic tube of the water/ nanofluids holding tank bottom outlet to connect the MT inlet. The copper sump that used has inner diameter 3 mm that connected to the tube and outer diameter 9.525 mm that connected to the plastic tube. Pressure gauge was fitted to the sump to measure the pressure inlet and outlet with a depth of 1 mm same as the inner diameter for the MT.

The heating on the tube wall was offered by an electrical AC power supply (0-220V– 25A). The heater wire surrounded the MT was used to heat up the MT wall. The heater temperatures range was from 0-100 °C.

The thermocouples used in the acquisition of measurements the walls, inlet and outlet temperature were type-k thermocouples. These thermocouples have insulation with a maximum allowable temperature of 200 °C. A subminiature plastic connector was attached to the thermocouple for easy connection to the data acquisition system.

To record all of the temperature data, three digital mini thermometer models 307/308 were used to acquire the thermocouple data. Each two thermocouples were connected to one mini thermometer. The mini thermometer model

307/308 recorded the temperatures in °C or °F with an accuracy of $\pm (0.3\% \text{ reading} + 1^\circ\text{C})$.

To measure the pressure drop between the MT inlet and outlet, an MD-S910 digital pressure gauge was used with an accuracy of $\pm 0.5\%$ of its full scale and pressure range of 0-15 bar. This pressure gauge was used to measure the pressure drop inside the MT between the inlet and outlet.

To measure the water/ nanofluids flow rate, a micro-flow meter omega (FTB 332) with outer diameter 3/8" was used. The flow rate range for this flow meter is 0.1 to 1 L/min (1.6 to 15.8 gph) with an accuracy of $\pm 6\%$ for its full scale. The flow rate could be calculated, and therefore the Reynolds number was calculated for measuring the water/ nanofluids velocity inside the MT.

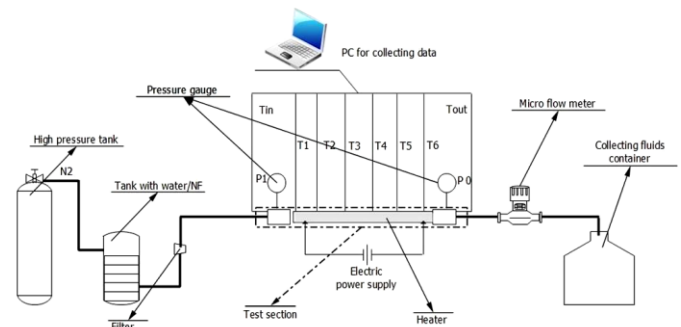


Figure 1: Schematic diagram of the experimental setup

2.2 EXPERIMENTAL PROCEDURE AND UNCERTAINTY ANALYSIS

The first step in conducting the experiments was to degas the fluid in the fluid holding tank. This was accomplished by letting some nitrogen flow into the tank while the cap of the tank was uncovered. Once the fluid was degassed, the fluid holding tank was sealed. The heater was turned on, and the temperature of the fluid was allowed to reach about 80°C. This temperature was monitored to ensure that it remained constant throughout the data taking process. The temperatures were measured from the mini thermometer, and once they reached a steady state value, the temperatures of the inlet, the outlet, and the walls were recorded. It should be noted that during the temperature measurement that all temperatures remained constant with time. Micro flow meter was placed on the test section outlet to calculate the fluid flow (controlling the velocity). This procedure was repeated several times at different temperatures and at different Reynolds numbers range. Different nanofluids such as Al₂O₃ and SiO₂ with different concentrations were tested.

Measurement accuracy is of crucial importance to ensure the validity of the test data. A standard uncertainty analysis was conducted for each measurement. The uncertainty of pressure measurements was found to be approximately 0.27% psi, the uncertainty of temperature measurements was found to be approximately 0.61% °C, and the uncertainty of flow rate

measurements was found to be less than 6 %. Using these uncertainties, an uncertainty analysis for uncorrected friction factor and Nusslet number based on propagation of errors was conducted. These uncertainties were calculated through the following formula [25]:

$$U_R = \left[\sum_{i=1}^n \left(\frac{\partial R}{\partial x_i} u_{xi} \right)^2 \right]^{1/2} \quad (2)$$

Where U_R is the uncertainty of value R and u_{xi} is the uncertainty of a given quantity x_i upon which R is based [25]. For Nusselt number, the x_i 's included q , d_h , l , $(T_{out} - T_{in})$, δt_x , k_1 . and the uncertainty in determining the friction factor consists of the uncertainties from Δp , d_i , v , L . this method of uncertainties determination allowed for the errors in each measurement to be compounded together to estimate the total error for Nusselt number and friction factor. The details of the related parameters uncertainties and the resulted uncertainties in friction factor, heat transfer coefficient and Nusselt number are listed in Table 3.

Table 3: The measurement uncertainties

| Parameters | Maximum uncertainty (%) |
|--------------|-------------------------|
| D_i | 1 |
| L | 0.95 |
| l | 0.4 |
| U | 0.3 |
| Δp | 0.3 |
| ΔT_x | 1.8 |
| c_p | 0.3 |
| ρ | 0.11 |
| v | 0.5 |
| m | 0.3 |
| k_1 | 1.2 |
| Re | 2.67 |
| f | 2.27 |
| h | 2.9 |
| Nu | 5.5 |

2.3 DATA REDUCTION METHOD

The heat applied to the working fluid in the microtube is obtained by [9]:

$$\Phi = U \cdot I \quad (3)$$

$$Q = m c_p (T_{out} - T_{in}) \quad (4)$$

where Φ is the power supply; U is the voltage supply and I is the electric current; \dot{m} is the mass flow rate and was measured from the volume of water collected from the outlet of the microtube over a specified period of time for low Reynolds number, and from the flow meter for high Reynolds number. The inlet temperature and outlet temperature were taken from the thermocouples inserted into the pressure tap tubes. It is noted again that the experimental condition was that of a constant heat flux for the walls of the microtube. Under this assumption, the average heat transfer coefficient for a microtube is given as follow:

$$q = \frac{Q}{A_W} = \frac{\dot{m} c_p (T_{out} - T_{in})}{\pi D_i L} \quad (5)$$

Where q : is the heat flux; Q : is the heat transfer rate; A_W : is the wall area.

The local heat transfer coefficient h_x and Nusselt number Nu_x are calculated by the following equations:

$$h_x = \frac{q L_x / L}{\Delta T_x} \quad (6)$$

$$Nu_x = \frac{h_x \cdot D_h}{k_1} = \frac{q \cdot \frac{L_x}{L} \cdot D_h}{\Delta T_x k_1} = \frac{\dot{m} c_p (T_{out} - T_{in}) D_h \cdot L_x / L}{A_W \Delta T_x k_1} \quad (7)$$

$$\Delta T_x = T_{wx} - T_{b,x,int} \quad (8)$$

$$T_{b,x,int} = T_{in} + \frac{Q \cdot L_x / L}{m c_p} \quad (9)$$

As can be seen in Eqs. (7) and (8), to calculate the local heat transfer coefficient and Nusselt number, the water bulk temperature $T_{b,x,int}$ distribution along the axial direction must be obtained. It is difficult to measure the fluid bulk temperature directly during the experiments. For the conventional size tube, a linear interpolation of the fluid bulk temperature shown by eq. (9) is adopted.

For the pressure drop measuring the pressure drop from the inlet and the outlet, the apparent Darcy friction factor (f) could be determined as follow:

$$f_{app,u} = \Delta p \cdot \frac{D_i}{L} \cdot \frac{2}{\rho u_{ave}^2} \quad (10)$$

Where Δp is the pressure drop that was measured in the experiments. The Δp is obtained by as follow:

$$\Delta p = \Delta p_{in,out} - \rho_d \quad (11)$$

$$\rho_d = 1.18 \rho u_{ave}^2 \quad (12)$$

$$u_{ave} = \frac{\dot{m}}{\rho A_{c,in}} = \frac{4\dot{m}}{\rho \pi D_i^2 v} \quad (13)$$

$$Re = \frac{u_{ave} \cdot D_i}{\nu} = \frac{4\dot{m}}{\rho \pi D_i^2 \nu} \quad (14)$$

Since the pressure was measured from the inlet and outlet, it is important to note that the apparent friction factor should not be confused with the fully developed Darcy friction factor, f (commonly referred to as simply the friction factor), which is

$$f = \frac{8 \tau_w}{\rho V_{ave}^2} \quad (15)$$

Where τ_w is the wall shear stress. To compare against the friction factor data obtained from the experiments. Equation (16) is used which involves fully developed flow in the laminar regime. For the fully developed friction factor for laminar flow in circular tube, an analytically derived equation is:

$$f = \frac{64}{Re} \quad (16)$$

In case of the assumption made that the flow entering the tube is uniform and the flow in the tube is completely laminar, the effect of the hydrodynamically developing region may be overestimated for the experimental cases. Both the assumptions of a uniform inlet and of fully laminar flow in the tube are questionable for the cases seen in the experiments.

3 RESULTS AND DISCUSSION

3.1 FLOW CHARACTERISTICS

According to Eqs. (10) to (15), the experimental friction factor for laminar flow was calculated for different types of working fluids such as pure water, Al₂O₃-water and SiO₂-water and at particle concentration of 1%. The Reynolds number used was ranged from 90 to 800. Figure 2 shows the friction factor for pure water and nanofluids with the conventional prediction. The experimental results show good agreement with the conventional theoretical values. The friction factor for SiO₂ has the higher values followed by Al₂O₃, pure water, respectively, this because SiO₂ has the highest pressure drop and the friction factor is proportional

directly with pressure drop values. Highest pressure drop leads to highest friction factor and vice versa.

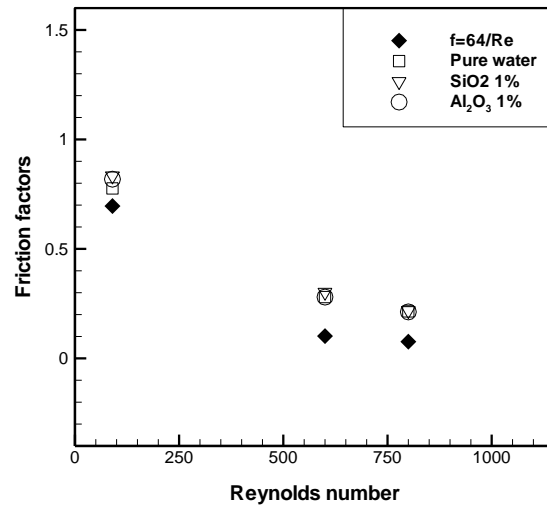
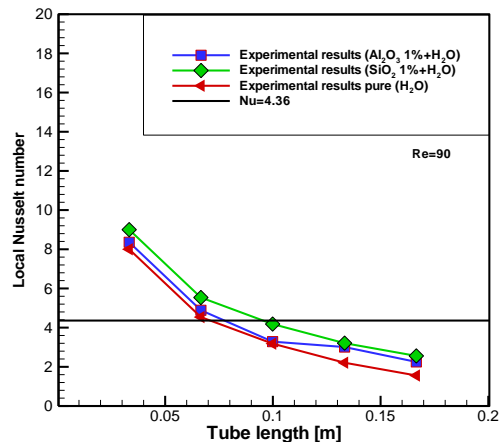


Figure 2: Friction factor for different types of fluids

3.2 HEAT TRANSFER CHARACTERISTICS

The experimental results for the effects of using different types of nanofluids on Nusselt number at different Reynolds number are presented in Figure 3a-c. This figure shows that SiO₂ has the highest Nusselt number followed by Al₂O₃ and pure water. The results were compared with the conventional theory for fully developed laminar flow at constant heat flux (Nu=4.36). It was found that the lower Reynolds number has the highest difference. As it can be seen in Figure 3 b, c that the values of local Nusselt number reached to the constant value of Nu=4.36 at higher Reynolds number. This could be a result of a number of cases. Beside experimental error, the biggest unknown in the present analysis is the type of flow regime that is present at each Reynolds number. Certainly if the flow is either transitional or turbulent at any given Reynolds number, it will not correlate with laminar developing flow Nusselt number correlations. It should be noted that there may be some effects from either the surface roughness or inlet condition at play here in the laminar regime.



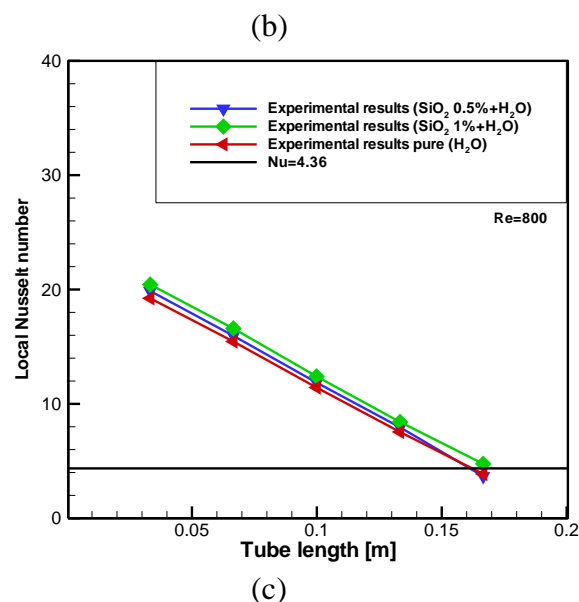
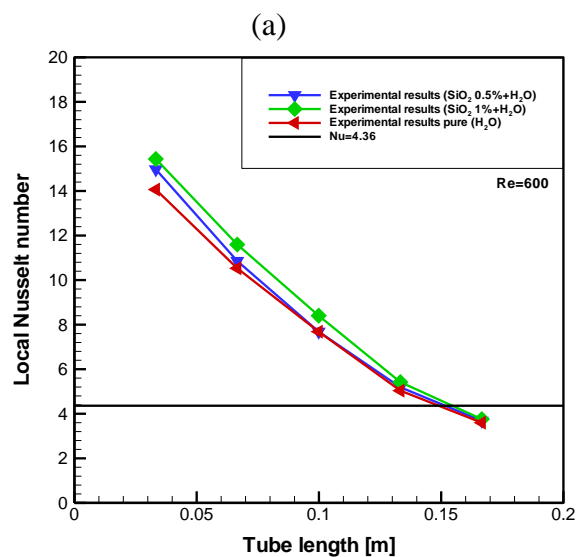
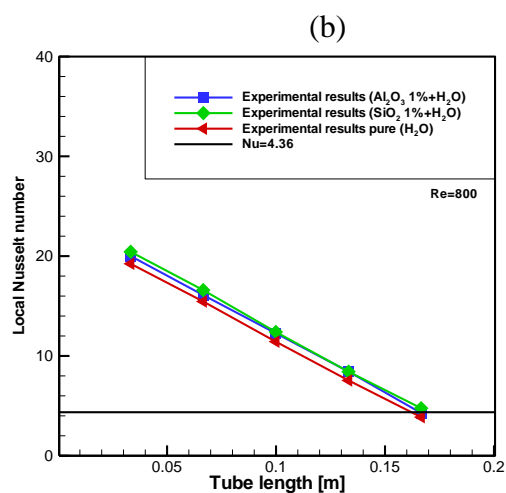
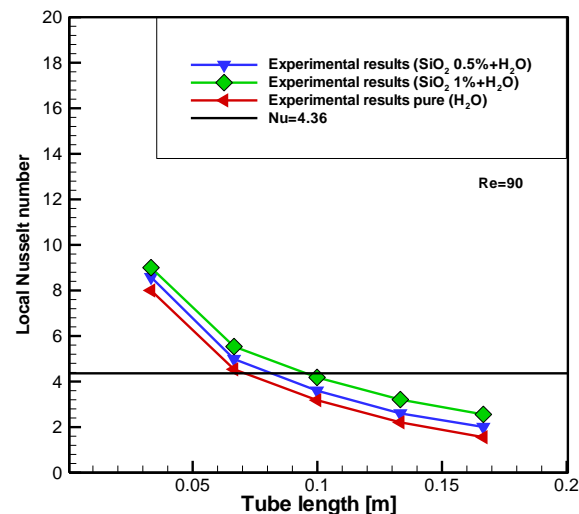
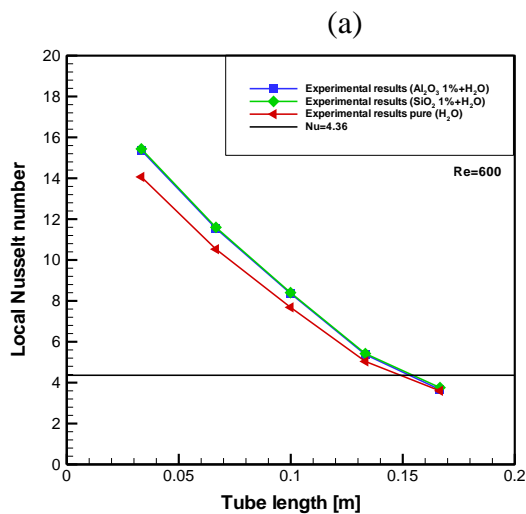


Figure 3: Local Nusselt number for different types of nanofluids at different Reynolds numbers: (a) $Re=90$; (b) $Re=600$; (c) $Re=800$.

After the results of effects of nanofluids showed that the SiO_2 has the highest Nusselt number, the effects of using different particle concentrations in preparing the nanofluids have been investigated as shown Figure 4. Two different particles ranged from 0.5 % to 1 % for SiO_2 . The results show that 1% SiO_2 has the highest Nusselt number followed by 0.5% particle concentration then the pure water. The reason for that is increasing the volume fraction leads to increase the density so the Prandtl number would increase and since the Nusselt number is a function of Prandtl number so the heat transfer would increase. The experimental results also revealed that using the nanofluids leads to enhance the heat transfer about 22% compared to conventional fluids like water. It is clear from Figure 4 a-c that the local Nusselt number increases as the Reynolds number increases.

Figure 4: Local Nusselt number for different nanoparticle concentration: (a) Re=90; (b) Re=600; (c) Re=800.

CONCLUSION

Forced laminar flow of water and nanofluids inside the microtube was experimentally studied. The nanofluids types used were Al₂O₃-water and SiO₂-water and the pure water. The nanoparticle concentration used was 0.5% to 1%. Reynolds number used was ranged from 90 to 800. The effects of nanofluids on the friction factor and the heat transfer rate were presented in this work. The results reveal that heat transfer was enhanced by using the nanofluid around 22% compared to the conventional fluids (water). The results show that the SiO₂ at 1% particle concentration has the highest Nusselt number and highest friction factor followed by Al₂O₃ then water.

REFERENCES

- [1] Yu W., France D.M., Routbort J. L., Choi S. U. S., Review and comparison of nanofluid thermal conductivity and heat transfer enhancements, *Heat Transfer Engineering*, Vol. 29, 2008, pp. 432–460.
- [2] Özerinç S., Kakaç S., Yazcolu A., Enhanced thermal conductivity of nanofluids: a state-of-the-art review, *Microfluidics and Nanofluidics*, Vol. 8, 2010, pp. 145–170.
- [3] Beck M.P., Yuan Y., Warriar P., Teja A.S., The effect of particle size on the thermal conductivity of alumina nanofluids, *Journal of Nanoparticle Research*, Vol. 11, 2009, pp. 1129–1136.
- [4] Mohammed H. A., Bhaskaran G., Shuaib N. H., Saidur R., Heat transfer and fluid flow characteristics in microchannels heat exchanger using nanofluids: a review, *Renewable and Sustainable Energy Reviews*, Vol. 15, 2011, pp. 1502–1512.
- [5] Chen H., Witharana S., Jin Y., Kim C., Ding Y., Predicting thermal conductivity of liquid suspensions of nanoparticles (nanofluids) based on rheology, *Particuology*, Vol. 7, 2009, pp. 151–157.
- [7] Salman B.H., Mohammed H.A., Kherbeet A. Sh., Heat transfer enhancement of nanofluids flow in microtube with constant heat flux, *International Communications in Heat and Mass Transfer*, Vol. 39, 2012, pp. 1195–1204.
- [8] Salman B.H., Mohammed H.A. Munisamy K.M., Kherbeet A.Sh, Characteristics of heat transfer and fluid flow in microtube and microchannel using conventional fluids and nanofluids: A review, *Renewable and Sustainable Energy Reviews*, Vol. 28, 2013, pp. 848–880
- [9] Liu Z.G., Liang S.Q., Takei M., Experimental study on forced convective heat transfer characteristics in quartz microtube, *International Journal of Thermal Sciences*, Vol. 46, 2007, pp. 139–148.
- [10] Li Z., He Y.L., Tang G.H., Tao W.Q., Experimental and numerical studies of liquid flow and heat transfer in microtube, *International Journal of Heat and Mass Transfer*, Vol. 50, 2007, 3447–3460.
- [11] Lelea D., Effects of temperature dependent thermal conductivity on Nu number behavior in micro-tubes, *International Communications in Heat and Mass Transfer*, Vol. 37, 2010, pp. 245–249.
- [12] Celata G.P., Cumo M., McPhail S., Zummo G., Characterization of fluid dynamic behavior and channel wall effects in microtube, *International Journal of Heat and Mass Transfer*, Vol. 27, 2006, pp. 135–143.
- [13] Hao P.F., Zhang X.W., Yao Z.H., He F., Transitional and turbulent flow in a circular microtube, *Experimental Thermal and Fluid Science*, Vol. 32, 2007, pp. 423–431.
- [14] Mala Gh.M., Li D., Flow characteristics of water in microtubes, *International Journal of Heat and Fluid Flow*, Vol. 20, 1999, pp. 142–148.
- [15] Wen D., Ding Y., Experimental investigation into convective heat transfer of nanofluids at the entrance region under laminar flow conditions, *International Journal of Heat and Mass Transfer*, Vol. 47, 2004, pp. 5181–5188.
- [16] Koo J., Kleinstreuer C., Viscous dissipation effects in microtubes and microchannels, *International Journal of Heat and Mass Transfer*, Vol. 47, 2004, pp. 3159–3169.
- [17] Lelea D., Cioabla A.E., The viscous dissipation effect on heat transfer and fluid flow in microtubes, *International Communications in Heat and Mass Transfer*, Vol. 37, 2010, pp. 1208–1214.
- [18] Minea A.A., Uncertainties in modeling thermal conductivity of laminar forced convection heat transfer with water alumina nanofluids, *Heat and Mass Transfer*, Vol. 68, 2014, pp. 78–84.
- [19] Minea A.A., Effect of microtube length on heat transfer enhancement of an water/Al₂O₃ nanofluid at high Reynolds numbers. *Heat and Mass Transfer*, Vol. 62, 2013, pp.22-30.
- [20] Kang S.W., Wei W.C., Tsai S.H., Huang C.C., Experimental investigation of nanofluids on sintered heat

pipe thermal performance. *Applied Thermal Engineering*, Vol. 29, 2009, pp. 973-979.

- [21] Moraveji M.K., Esmaili E., Comparison between single-phase and two-phase CFD modeling of laminar forced convection flow of nanofluids in a circular tube under constant heat flux. *Int. Comm. Heat and Mass Transfer*, Vol. 39, 2012, pp. 1297-1302.
- [22] Akbari M., Behzadmehr A., Shahraki F., Fully developed mixed convection in horizontal and inclined tubes with uniform heat flux using nanofluid. *Heat and Fluid Flow*, 29, 2008, pp. 545-556.
- [23] Wu Z., Wang L., Sundén B., Pressure drop and convective heat transfer of water and nanofluids in a double-pipe helical heat exchanger. *Applied Thermal Engineering*, Vol. 60, 2013, pp. 266-274.
- [24] Lee J, Mudawar I. Assessment of the effectiveness of nanofluids for single- phase and two-phase heat transfer in micro-channels, *International Journal of Heat and Mass Transfer*, Vol. 50(3-4), 2007, pp. 452-63.
- [25] Choi C., Yoo H.S., Oh J.M. Preparation and heat transfer properties of nanoparticle-in-transformer oil dispersions as advanced energy-efficient coolants. *Current Applied Physics*, Vol.8, 2008, pp.710-2.
- [26] Salman B.H., Mohammed H.A. Munisamy K.M., Kherbeet A.Sh. Three Dimensional Numerical Investigation of Nanofluids Flow in Microtube with Different Values of Heat Flux. *Heat Transfer-Asian Research*, 0(0), 2014